

# 870. Vibrational analysis of planetary gear trains by finite element method

Pei-Yu Wang<sup>1</sup>, Xuan-Long Cai<sup>2</sup>

Department of Mechanical Design Engineering, National Formosa University

Yun-Lin County, 632, Taiwan, R. O. C.

E-mail: <sup>1</sup>wangpy@nfu.edu.tw, <sup>2</sup>free77118@gmail.com

(Received 11 September 2012; accepted 4 December 2012)

**Abstract.** Planetary gear trains produce several advantages, including high speed reduction, compactness, greater load sharing and higher torque to weight ratio, which are used widely in wind turbine, automobiles, robot and other applications. In some important transmission applications, the noise and vibration are key concerns in design. In this paper, a 3D dynamic contact and impact analysis model of planetary gear trains has been proposed. Tooth surface friction, backlash, tolerance of peg hole, and time-varying stiffness were considered in this dynamic model. The ANSYS / LS-DYNA were utilized to analyze the dynamic responses of gear transmission of the planetary gears. The vibration behavior of an actual gear set under dynamic loading was simulated in the dynamic model. The stiffness and elastic deformation of gear teeth are calculated using the finite element method with actual geometry and positions of the gears. The time-varying position of the carrier defined as the vibration and noise source. After impact analysis, the numerical results of vibration of carrier involved with the transient and steady states. Through the Fast Fourier Transform (FFT) methods, frequency spectrums of the transient and steady states of the calculated vibration of planet carrier are obtained for the gearbox designer to avoid the resonance zone.

**Keywords:** planetary gear trains, impact, dynamic, FFT.

## Introduction

Regarding the correct analysis of gear transmission, the primary condition is that the components of the gear transmission must be analyzed separately. This method deconstructs a complicated problem into several problems that are relatively simple to solve. However, during the decomposition process, several mutually influential factors must be considered. Additionally, only by identifying the primary influential factor can accurate results be achieved. Oguz Kyabasi [1] used experimental analysis to calculate the stress load distribution on the outline of the tooth surface. Cai and Gayashi [2] used a spur gear dynamics equation that was similar to a linear equation instead of a non-linear single degree of freedom kinetic equation; their analysis and experimental results were roughly consistent. Research of the dynamic characteristics of planetary gear systems involves calculating the natural frequency of the system, vibration mode, dynamic deformation, and dynamic power [3-7]. However, August and Kasuba [8] considered the influence of changes in the gear meshing rigidity and sun gear fixed method on the dynamic power of planetary gear systems and identified the relatively superior properties of fixed sun gear design. Vexel and Flamand [9] also obtained the same results. When considering time variation, Tordionhe and Gauvin [10] investigated the dynamic stability of two planetary geared systems. Recent literature [11] analyzes multistage planetary wheel gear system dynamics, exploring the natural frequencies and vibration modes of 10 types of planetary gear systems.

Wear in the gear design, backlash, contact ratio and gear tooth strength are important parameters that influence the gear. Use optimum gear modification and teeth trimming gear design methods has become an important strategy to improve the performance of gears. Because the planetary gear has numerous teeth, which have a complicated structure, the gear center distance is subject to greater restrictions and is difficult to adjust. Therefore, the focus of gear design is the matching of the gear strength and the contact rate, and using tip relief methods to improve the

dynamic characteristics and life expectancy of planetary gear systems. Arikan [12] discussed the modification coefficients, backlash, gear center distance and undercutting, line of action, and tooth surface meshing characteristics of cylindrical gear systems. Shuting Li [13] investigated the difference between the theoretical planetary gear contact problem method and numerical analysis, using finite element software to simulate the three-dimensional contact analysis and load distribution of the gear. Abousieiman [14] combined the integral method with the simultaneously occurring meshing contact algorithm to solve the motion equation of the dynamic operation of spur and helical gears, proposing an effective formula for analyzing flank modifications and errors.

## Research method

### Finite element method

The finite element method (FEM) is a common analysis method. This study focuses on dynamic nonlinearity analysis, and uses LS-DYNA to solve the problems of large non-linear transient dynamic displacement and deformation. When solving dynamic problems, the time must be divided into numerous sections and the physical quantities in time  $t + \Delta t$  must be obtained based on the physical quantities in time  $t$ . In the program, the method used for integrating time is primarily the central difference method, which is an explicit integration. Explicit integration is an integral method with conditional stability and can be applied to physical problems of rapid dynamic loading and highly nonlinear behavior. In addition, explicit integration does not perform iterations during the solving process. The advantages of this method are that no convergence issues or demand to solve simultaneous equations exists; however, the disadvantage is that an extremely small time step is required for stability. Therefore, to ensure the program is executed correctly, the size of the increment time must be considered during the analysis. The Newmark Method algorithm proposed by Hughes (1987) is also used frequently. This algorithm integrates time for the discrete equations of motion and describes the discrete equations of motion [15] in a linear mass-spring-damper system using a simple single degree of freedom:

$$m\ddot{u} + c\dot{u} + ku = p(t) \quad (1)$$

$\ddot{u}$  is acceleration,  $\dot{u}$  is velocity,  $u$  is displacement,  $p(t)$  is the external force,  $m$  is the mass,  $c$  is damping coefficient, and  $k$  is the stiffness matrices.

If  $m$ ,  $c$  and  $k$  are constant, (1) is linear. Therefore, the ordinary differential equations can be solved using the analysis method. For nonlinear problems,  $k$  is a function of the displacement  $u$ . Thus, (1) can be expressed as:

$$m\ddot{u} + c\dot{u} + k(u)u = p(t) \quad (2)$$

Although obtaining the analytical solution of (2) is difficult, the numerical solution can be obtained. The methods commonly used for this are the finite difference method and the finite element method. Regarding the finite element method, the matrix form of the above equation of motion is:

$$M\ddot{U} + C\dot{U} + KU = P(t) \quad (3)$$

In (3),  $U$  is the displacement matrix,  $\dot{U}$  is the node velocity matrix,  $\ddot{U}$  is the node acceleration matrix,  $M$  is the mass matrix,  $C$  is the damping coefficient matrix,  $K$  is the stiffness matrix, and  $P(t)$  is the external force vector matrix.

There are two common methods for solving (3), one is the mode superposition method and the other is step-by-step integration. For complex problems, step-by-step integration is generally adopted. The step-by-step integration method can be broadly divided into the increment method, the iterative method, and the mixing method. The method commonly used to solve problems is the increment iterative method, where the stiffness matrices must be replaced, and the solutions archived through a series of linear approximations (the Newton-Raphson). However, when solving problems of highly nonlinear dynamics for internal contact, convergence often cannot be guaranteed. Therefore, LS-DYNA uses the explicit central difference method to integrate time.

### Finite element model of the micro planetary gear

In this paper, the analyzed elements of gears in the 3D dynamic contact/impact FE model are created by using C++ program directly to obtain high meshing quality as shown in Fig. 1. First, the true gear tooth surfaces that calculated by differential geometry theory were imported into the Pro/ENGINEER software to create the three-dimensional model of the planetary gears. The design parameters of the planetary gears were listed in Table 1. Then, the finite element model grids of the planetary gears were created by HyperMesh software. The ANSYS/LS-DYNA software is used to solve the dynamic responses of carrier run out after allotting suitable materials, boundary conditions, and other required settings.

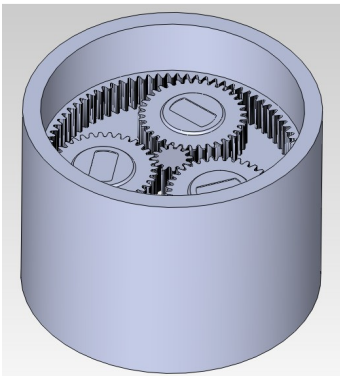


Fig. 1. The micro planetary gears model

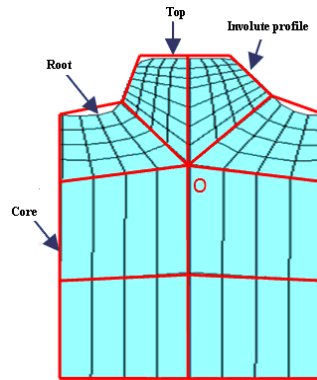


Fig. 2. The grids delimitation of the gear model

Table 1. The design parameters of the planetary gears

	Sun	Planet	Ring
Modulus	0.25 mm		
No. of teeth	12	35	81
Pressure ang.	20 Degree		
Coefficient of add.	0		
Center dis.	5.875 mm		

To produce a high-quality finite element grid, with an easily adjustable density and distribution, the tooth of the planetary gear must be divided into multiple quadrilateral blocks. With the involute profile of the tooth and the starting point of the tooth root fillet, a reference point

O in the middle of the tooth surface is set as the basis for segregating the tooth surface area by dividing the blocks into quadrilateral areas, as shown in Fig. 2.

The analytic accuracy of the meshing gears depends on the number of grids, which distribute the working area (involute profile) and the tooth root fillet. Therefore, the finite element model with the appropriate grid density, not only can the precision of the finite element model be enhanced, but the analysis time can also be reduced.

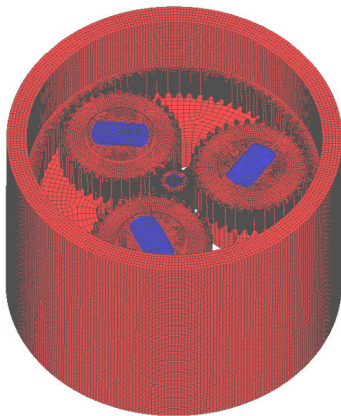
### Mechanical property settings for the material in the micro planetary finite element model

The micro planetary gears model used in this study include (1) a sun gear; (2) three planets; (3) a ring gear; (4) a carrier; and (5) three planetary axles (as shown in Fig. 1). The sun gear meshes simultaneously with the three planets, while the three planets mesh with the ring gear, which means that the model of the entire gear has six mesh points during every movement. In this model, the backlash is set to 0.05 mm, and the assembly clearance between planetary axles and planetary gear holes is set to 0.02 mm. A compact gear box was considered, the ball bearing design was not adopted for the micro planetary gear model. When a mutual rotational motion relationship exists between two model components in this study, medium-carbon steel (S45C) and copper are selected for the materials to reduce the friction between the two contact surfaces. In this model, copper material was set to the carrier. Medium-carbon steel (S45C) was also selected for the three planetary axles. The material for the remaining components was also medium-carbon steel (S45C) because of consideration of its strength, Table 2 shows it.

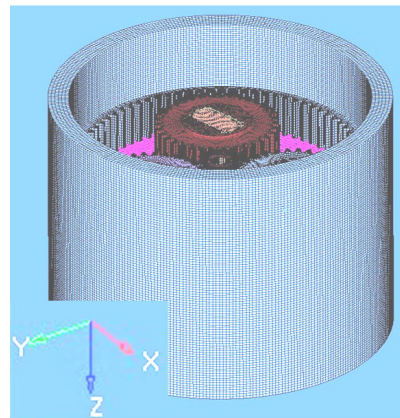
**Table 2.** Mechanical properties of the applied materials

Material	Density (g/cc)	Tensile strength (MPa)	Yield point (MPa)	Young's modulus (GPa)	Poisson's ratio
S45C	7.85	569	343	205	0.29
COPPER	8.93	210	33.3	110	0.343

In the explicit dynamics software LS-DYNA, because speed and torque must be defined in the rigid body, the materials in the models should be divided into two material properties: rigid body and plastic body, respectively. The rigid body drives the plastic body to rotate (the rigid and plastic bodies are marked in red ■ and blue ■, respectively); thus, the material property parameters should be inputted as shown in Fig. 3. The properties of materials and elements in the model are shown in Table 3.





**Fig. 3.** The planetary gears model



**Fig. 4.** The axis of the rotating coordinate system

**Table 3.** The element properties applied in this study

Material properties	Core elements	Plastic body (*MAT_PIECEWISE_LINEAR_PLASTICITY)	
	Axial elements	Rigid body (*MAT_RIGID)	
Element properties	Three-dimensional	3D body element (*SECTION_SOLID)	--

**Boundary condition settings of the micro planetary gear**

During the meshing transmission process of the micro planetary gear in this study, the sun gear acts as the driving gear at a specific constant speed, causing the planetary gear to revolve and rotate. By contrast, the ring gear does not move and the planetary gear drives the planetary shaft to revolve and rotate. Finally, the planetary shaft drives the carrier to produce a rotation output. Therefore, the sun gear is set to possess an angular velocity and torque. Because the driven gears must achieve a balance of torque with driving gears, the driven gears should include an anti-torque mechanism to counterbalance the driving gears. The planetary gear transmits torque through the tooth contact; the torque is calculated with an input power of 10 watts (W).

In the HyperMesh preprocessor, the boundary constraints and loading are set on the rigid body. Therefore, for the driving gears, a rotational speed can be defined in the internal elements of the rigid body and a driving torque is applied. For driven gears, an anti-torque mechanism is defined in the inner elements of the rigid body, causing the gears to perform a rotational motion. The constraint displacement and rotation parameter conditions are determined by the axis of the rotating coordinate gear system. The axis of the rotating coordinate system, on which the micro planetary rotates, is shown in Fig. 4. The constrained parameters are shown in Table 4.

**Table 4.** Constraint settings of the component parts

	Constraints of displacement	Constraints of rotation
Axis elements of sun gear (rigid body)	$x, y, z$	$A, B$
Axis elements of planet gear (rigid body)	$z$	$A, B$
Axis elements of ring gear (rigid body)	$x, y, z$	$A, B, C$
Axis elements of carrier (rigid body)	$z$	$A, B$

The contact method in this study is the penalty function method. The basic principle of this method is explained below. First, in each time step, before changing the displacements of nodes, each slave node is checked to determine whether they have penetrated the master surface. Slave nodes that have not penetrated the master surface are not processed. Alternatively, if the slave nodes have penetrated the master surface, a larger interface contact force is introduced between the slave nodes and the master surface. The size of this force is proportional to the penetration depth and the stiffness of the master surface, which is equivalent to placing a normal spring between the slave nodes and the master surface to prevent the nodes from penetrating the master surface.

To comprehensively describe the interaction between objects of complex geometry under a large deformation contact and power impact, LS-DYNA possesses numerous contact types. During the analysis procedure, no contact element exists. After identifying the surfaces likely to contact, their contact types, and a number of parameters regarding the contact, the contact surfaces can be ensured not to penetrate the contact interface during program calculations, and the function of friction during relative motion of the contact interfaces can be considered. The contact type adopted in this study was the "automatic surface-to-surface contact" of two-way contact (\*CONTACT\_AUTOMATIC\_SURFACE\_TO\_SURFACE). This contact type automatically

detects any collision between objects on both sides and is easy to define. However, when defining contacts, including all objects is not necessary, only the object elements with contact should be included. In addition to the CPU computation time, the search time for contact during analysis can be reduced.

### Simulation results of the micro planetary gears contact/impact analysis

Fig. 5 shows the three-dimensional model of the planetary gear box. In this study, the driving sun gear set with power 10 watts and rotational speed 10,000 R. P. M. is used. Fig. 6 shows a planet gear, along the tooth profile direction three nodes were chosen to compare the effective stress of transient state with steady state. Fig. 7 shows the variation of the effective stress of the chosen three nodes during the transient state. Here, we can find an interesting condition, that the stress only appears at the instantaneous impact time. Fig. 8 shows the variation of the effective stress of the chosen three nodes during the steady state. The effective stress of the chosen three nodes change gradually during the meshing. Comparing the maximum effective stress of the transient with steady state, the amount of stress reduce from 85 MPa to 35 MPa. The amount of effective stress during the transient meshing is about 2.43 times then steady meshing. Fig. 9 shows the effective stress distribution on three teeth of sun gear, which located at the same radius. The amount of stress were 110 MPa, 75 MPa, and 85 MPa related to point A, B, and C, respectively. The main reason for the differential stress on symmetrical location was the vibration of the carrier.

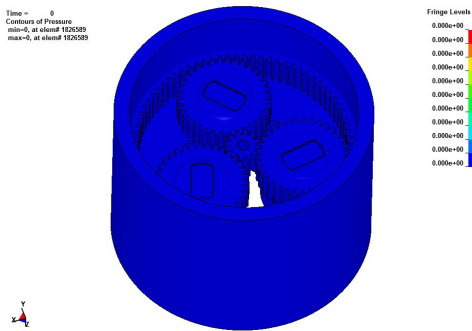


Fig. 5. The three-dimensional model of the planetary gear box

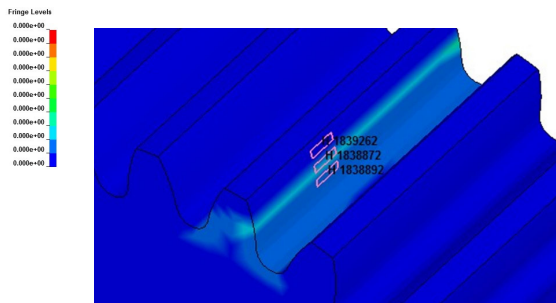


Fig. 6. The position of the chosen three nodes for stress comparison

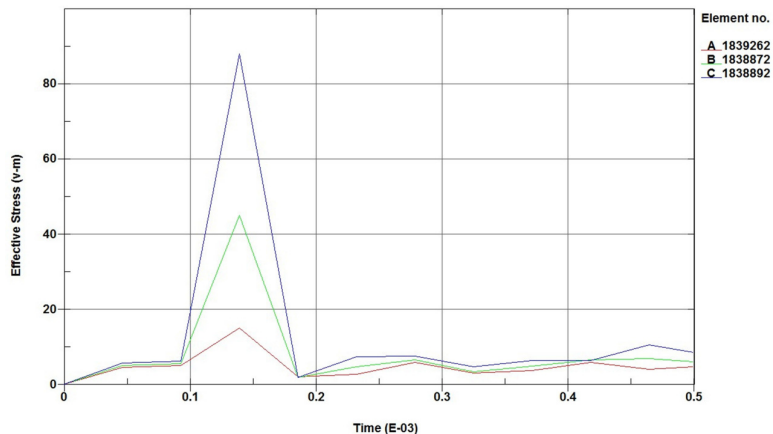


Fig. 7. The effective stress of the chosen three nodes during the transient state

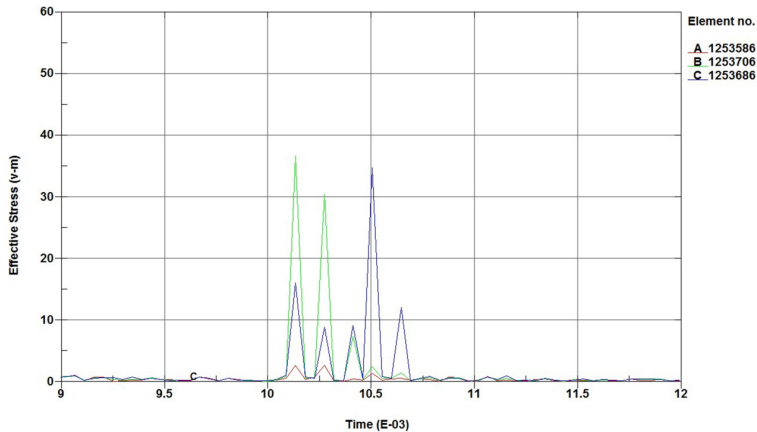


Fig. 8. The effective stress of the chosen three nodes during the steady state

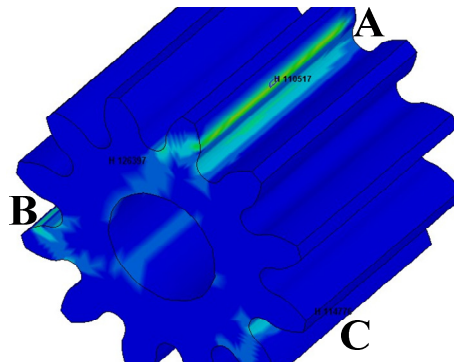


Fig. 9. The effective stress distribution on three teeth of sun gear

Choosing an arbitrary fixed node from the planetary carrier as the reference point, and the distance between the reference point and the rotation axis of sun gear set as a benchmark radius  $R^{(0)}$  at time  $t = 0$ , Fig. 12. During the motion of planetary gear, the position vector of the reference point is obtained and the corresponding radius  $R^{(t)}$  is calculated. The radius variation  $\Delta R^{(t)}$  of the reference point in the motion process is defined as vibration source of the gear box and expressed as follows:

$$\Delta R^{(t)} = R^{(t)} - R^{(0)} = \sqrt{x_t^2 + y_t^2} - R^{(0)} \quad (4)$$

where  $\{x_t, y_t\}$  expressed as the coordinate of reference point during the motion at arbitrary time  $t$ . Then, the carrier runout with time domain can be obtained, as shown in Fig. 10. By Fast Fourier Transform method, the carrier runout time domain will be transfer to the frequency response spectrum, as shown in Fig. 11.

## Conclusion

In this study, a three-dimensional dynamic contact/impact analysis model of the micro-planetary gears was proposed. The real tooth surfaces of the planetary gears were calculated



by differential geometry algorithm and the three-dimensional model was produced by Pro/Engineer software. The three-dimensional model was imported into the HyperMesh preprocessor to set up grid mesh. In this analysis model, elastic materials, contact/impact type, the friction force between two mating gear surfaces, tolerance of peg holes of the axle of planet gear, and backlash were considered. Here, we obtain position vectors (run-out) of the carrier during the motion of planetary gears by the calculation of the LS-DYNA software. Finally, by using the FFT technology, the run-out of the carrier with time domain was transformed into a frequency spectrum for gearbox designer to avoid the resonance region.

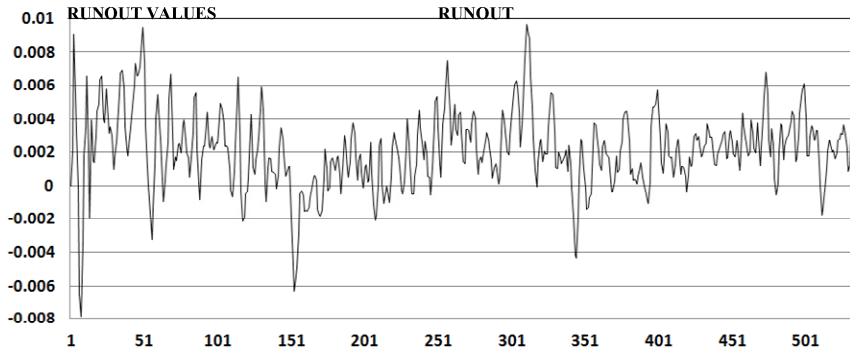


Fig. 10. The carrier runout with time domain

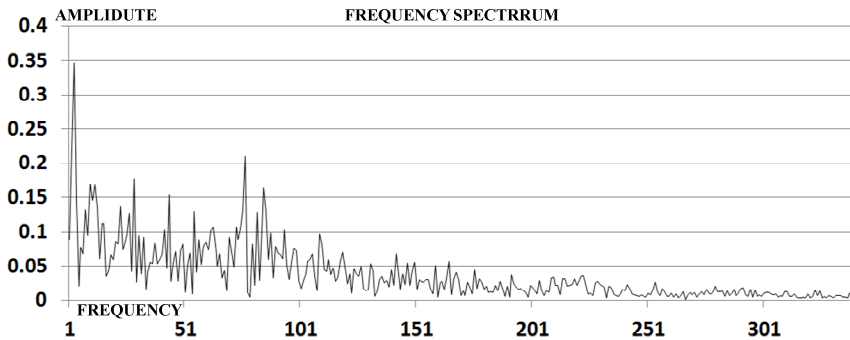


Fig. 11. The frequency response spectrum of the carrier

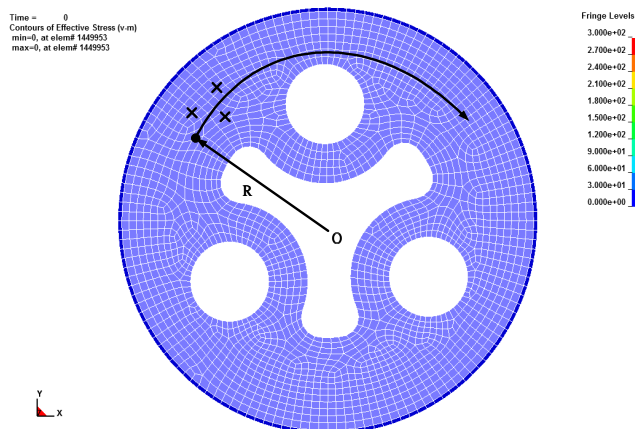


Fig. 12. The reference point on the carrier



## Acknowledgments

The authors thank the Precision Machinery Research and Development Center for financial support.

## References

- [1] **Oguz Kayabasi** Shape optimization of tooth profile of a flex spline for a harmonic drive by finite element modeling. *Materials & Design*, Vol. 28, Issue 2, 2007, p. 447.
- [2] **Y. Cai, T. Hayashi** The linear approximated equation of vibration of a pair of spur gears-theory and experiment. *Transactions of ASME, Journal of Mechanical Design*, 1994, p. 558-564.
- [3] **F. Cunliffe, J. D. Smith, D. B. Welbourn** Dynamic tooth loads in epicyclic gears. *ASME Journal of Engineering for Industry*, 1974, p. 578-584.
- [4] **D. L. Seager** Conditions for the neutralization of excitation by the teeth in epicyclic gearing. *Journal of Mechanical Engineering Science*, Vol. 17, 1975, p. 293-298.
- [5] **M. Botman** Epicyclic gear vibrations. *ASME Journal of Engineering for Industry*, 1976, p. 811-815.
- [6] **T. Hidaka, Y. Terauchi, K. Nagamura** Dynamic behavior of planetary gear – 5th report, dynamic increment of torque. *Bulletin of the JSME*, Vol. 22, 1979, p. 1017-1025.
- [7] **T. Hidaka, Y. Terauchi, K. Nagamura** Dynamic behavior of planetary gear – 6th report, displacement of sun gear and ring gear. *Bulletin of the JSME*, Vol. 22, 1979, p. 1026-1033.
- [8] **R. August, R. Kasuba** Torsional vibrations and dynamic loads in a basic planetary gear system. *ASME Journal of Vibration, Acoustics, Stress and Reliability in Design*, Vol. 108, 1986, p. 348-352.
- [9] **P. Velez, L. Flamand** Dynamic response of planetary gear trains to mesh parametric excitations. *ASME Journal of Mechanical Design*, Vol. 118, 1996, p. 7-14.
- [10] **G. V. Tordion, R. Gouvin** Dynamic stability of a two-stage gear train under the influence of variable meshing stiffness. *ASME Journal of Engineering for Industry*, 1997, p. 785-791.
- [11] **A. Kahraman** Free torsional vibration characteristics of compound planetary gear sets. *Mechanism and Machine Theory*, Vol. 36, 2001, p. 953-971.
- [12] **S. Arikian** Determination of addendum modification coefficients for spur gears operating at non-standard center distances. *Proceedings of the ASME, Design Engineering Technical Conference*, Vol. 4 A, 2003, p. 489-499.
- [13] **Shuting Li** Contact problem and numeric method of a planetary drive with small teeth number difference. *Mechanism and Machine Theory*, Vol. 43, 2008, p. 1065-1086.
- [14] **V. Abousleiman, P. Velez** A hybrid 3D finite element/lumped parameter model for quasi-static and dynamic analyses of planetary/epicyclic gear sets. *Mechanism and Machine Theory*, Vol. 41, 2006, p. 725-748.
- [15] Version 971, *LS-DYNA Keyword User's Manual*. Livermore Software Technology Corporation, 2007.